



**HAL**  
open science

# **Apatite (U-Th)/He Thermochronology Evidence for Two Cenozoic Denudation Events in the Eastern Part of the Sulu Orogenic Belt.**

Li Xu, Wu Lin, Marc Jolivet, Chang'An Li, Haijin Liu

► **To cite this version:**

Li Xu, Wu Lin, Marc Jolivet, Chang'An Li, Haijin Liu. Apatite (U-Th)/He Thermochronology Evidence for Two Cenozoic Denudation Events in the Eastern Part of the Sulu Orogenic Belt.. *Earth Science*, 2022, 47 (4), 16 p. <10.3799/dqkx.2019.000>. <insu-03601008>

**HAL Id: insu-03601008**

**<https://insu.hal.science/insu-03601008v1>**

Submitted on 8 Mar 2022

**HAL** is a multi-disciplinary open access archive for the deposit and dissemination of scientific research documents, whether they are published or not. The documents may come from teaching and research institutions in France or abroad, or from public or private research centers.

L'archive ouverte pluridisciplinaire **HAL**, est destinée au dépôt et à la diffusion de documents scientifiques de niveau recherche, publiés ou non, émanant des établissements d'enseignement et de recherche français ou étrangers, des laboratoires publics ou privés.



HAL Authorization

# 1 苏鲁造山带东段新生代两阶段剥露事件的磷灰石 (U-Th)/He 热年代学

## 2 证据

3 林旭<sup>1,2,4</sup>, 吴林<sup>2</sup>, Jolivet Marc<sup>3</sup>, 李长安<sup>4</sup>, 刘海金<sup>5</sup>

41. 三峡大学, 宜昌 276005

52. 中国科学院地质与地球物理研究所, 北京 100029

63. 法国雷恩第一大学, 雷恩

74. 中国地质大学(武汉), 武汉 430074

85. 东华理工大学, 南昌 330013

9

10 **摘要:** 苏鲁造山带位于华北和华南板块之间, 是中国东部最显著的陆内造山带之一, 约束其新  
11 12 13 14 15 16 17 18  
19 20 21 22 23 24 25 26 27  
28 29 30 31  
32 33 34 35 36 37 38 39 40  
41 42 43 44 45 46 47 48 49 50  
51 52 53 54 55 56 57 58 59 60  
61 62 63 64 65 66 67 68 69 70  
71 72 73 74 75 76 77 78 79 80  
81 82 83 84 85 86 87 88 89 90  
91 92 93 94 95 96 97 98 99 100  
101 102 103 104 105 106 107 108 109 110  
111 112 113 114 115 116 117 118 119 120  
121 122 123 124 125 126 127 128 129 130  
131 132 133 134 135 136 137 138 139 140  
141 142 143 144 145 146 147 148 149 150  
151 152 153 154 155 156 157 158 159 160  
161 162 163 164 165 166 167 168 169 170  
171 172 173 174 175 176 177 178 179 180  
181 182 183 184 185 186 187 188 189 190  
191 192 193 194 195 196 197 198 199 200  
201 202 203 204 205 206 207 208 209 210  
211 212 213 214 215 216 217 218 219 220  
221 222 223 224 225 226 227 228 229 230  
231 232 233 234 235 236 237 238 239 240  
241 242 243 244 245 246 247 248 249 250  
251 252 253 254 255 256 257 258 259 260  
261 262 263 264 265 266 267 268 269 270  
271 272 273 274 275 276 277 278 279 280  
281 282 283 284 285 286 287 288 289 290  
291 292 293 294 295 296 297 298 299 300  
301 302 303 304 305 306 307 308 309 310  
311 312 313 314 315 316 317 318 319 320  
321 322 323 324 325 326 327 328 329 330  
331 332 333 334 335 336 337 338 339 340  
341 342 343 344 345 346 347 348 349 350  
351 352 353 354 355 356 357 358 359 360  
361 362 363 364 365 366 367 368 369 370  
371 372 373 374 375 376 377 378 379 380  
381 382 383 384 385 386 387 388 389 390  
391 392 393 394 395 396 397 398 399 400  
401 402 403 404 405 406 407 408 409 410  
411 412 413 414 415 416 417 418 419 420  
421 422 423 424 425 426 427 428 429 430  
431 432 433 434 435 436 437 438 439 440  
441 442 443 444 445 446 447 448 449 450  
451 452 453 454 455 456 457 458 459 460  
461 462 463 464 465 466 467 468 469 470  
471 472 473 474 475 476 477 478 479 480  
481 482 483 484 485 486 487 488 489 490  
491 492 493 494 495 496 497 498 499 500  
501 502 503 504 505 506 507 508 509 510  
511 512 513 514 515 516 517 518 519 520  
521 522 523 524 525 526 527 528 529 530  
531 532 533 534 535 536 537 538 539 540  
541 542 543 544 545 546 547 548 549 550  
551 552 553 554 555 556 557 558 559 560  
561 562 563 564 565 566 567 568 569 570  
571 572 573 574 575 576 577 578 579 580  
581 582 583 584 585 586 587 588 589 590  
591 592 593 594 595 596 597 598 599 600  
601 602 603 604 605 606 607 608 609 610  
611 612 613 614 615 616 617 618 619 620  
621 622 623 624 625 626 627 628 629 630  
631 632 633 634 635 636 637 638 639 640  
641 642 643 644 645 646 647 648 649 650  
651 652 653 654 655 656 657 658 659 660  
661 662 663 664 665 666 667 668 669 670  
671 672 673 674 675 676 677 678 679 680  
681 682 683 684 685 686 687 688 689 690  
691 692 693 694 695 696 697 698 699 700  
701 702 703 704 705 706 707 708 709 710  
711 712 713 714 715 716 717 718 719 720  
721 722 723 724 725 726 727 728 729 730  
731 732 733 734 735 736 737 738 739 740  
741 742 743 744 745 746 747 748 749 750  
751 752 753 754 755 756 757 758 759 760  
761 762 763 764 765 766 767 768 769 770  
771 772 773 774 775 776 777 778 779 780  
781 782 783 784 785 786 787 788 789 790  
791 792 793 794 795 796 797 798 799 800  
801 802 803 804 805 806 807 808 809 810  
811 812 813 814 815 816 817 818 819 820  
821 822 823 824 825 826 827 828 829 830  
831 832 833 834 835 836 837 838 839 840  
841 842 843 844 845 846 847 848 849 850  
851 852 853 854 855 856 857 858 859 860  
861 862 863 864 865 866 867 868 869 870  
871 872 873 874 875 876 877 878 879 880  
881 882 883 884 885 886 887 888 889 890  
891 892 893 894 895 896 897 898 899 900  
901 902 903 904 905 906 907 908 909 910  
911 912 913 914 915 916 917 918 919 920  
921 922 923 924 925 926 927 928 929 930  
931 932 933 934 935 936 937 938 939 940  
941 942 943 944 945 946 947 948 949 950  
951 952 953 954 955 956 957 958 959 960  
961 962 963 964 965 966 967 968 969 970  
971 972 973 974 975 976 977 978 979 980  
981 982 983 984 985 986 987 988 989 990  
991 992 993 994 995 996 997 998 999 1000

18 **关键词:** 苏鲁造山带, 磷灰石, 隆升, (U-Th)/He 热年代学

## 19 Apatite (U-Th)/He thermochronology evidence for two Cenozoic denudation

## 20 events in the eastern part of the Sulu orogenic belt

21 Lin Xu<sup>1,2,4</sup>, Wu Lin<sup>2</sup>, Jolivet Marc<sup>3</sup>, Li Chang'an<sup>4</sup>, Liu Haijin<sup>5</sup>

221. *China Three Gorges University, Yichang 276005, China*

232. *Institute of Geology and Geophysics, Chinese Academy of Sciences, Beijing 100029, China*

243. *Univ Rennes, CNRS, Géosciences Rennes, UMR6118, CNRS – F-35000 Rennes, France*

254. *China University of Geosciences, Wuhan 430074, China*

265. *East China Institute of Technology, Nanchang 330013, China*

27

28 **Abstract:** The Sulu orogenic belt, located between the North China and South China plates, is one of  
29 the most prominent intracontinental Cenozoic orogenic belt in eastern China. Therefore, the  
30 denudation history of the Sulu orogenic belt provides significant insight into the basins-ranges  
31 evolution in eastern China and their driving geodynamic mechanism. The low closure temperature (ca.

1<sup>1</sup> 基金项目: 国家自然科学基金 (41972212); 湖南省自然科学基金项目(2019JJ40198)

2 第一作者简介: 林旭(1984-), 男, 副教授, 主要从事造山带隆升和中国大河演化研究。E-mail:

3 hanwuji-life@163.com

4 通讯作者: 李长安(1956-), 男, 教授, 主要从事长江演化与第四纪地质学的科研与教学工作。E-mail:

5 chanli@cug.edu.cn

3270°C) of the apatite (U-Th)/He system allows accurate constraint of the cooling processes of  
33 geological bodies in the upper crust. In this study, the apatite (U-Th)/He method was used to analyze  
34 the exhumation time of rocks on the Duofu and Juchi Mountains, eastern Sulu orogenic belt. The  
35 apatite (U-Th)/He age-elevation relationship and thermal history simulation results showed that the  
36 exhumation occurred in the Early-Middle Eocene (54-43 Ma) and Oligocene (35-27 Ma) for the  
37 Duofu and Juchi Mountains, respectively. These cooling episodes were synchronous to the  
38 exhumation of the western part of the Sulu orogenic belt. Combined with the results previously  
39 available in the region, it is shown that the geodynamics of eastern China was influenced by the  
40 Pacific plate subduction underneath eastern Asia. Extensive exhumation occurred in the early  
41 Cenozoic, which established the basin-mountain distribution pattern during this time.

42 **Key Words:** Sulu orogenic belt, Uplift, Apatite (U-Th)/He thermochronology

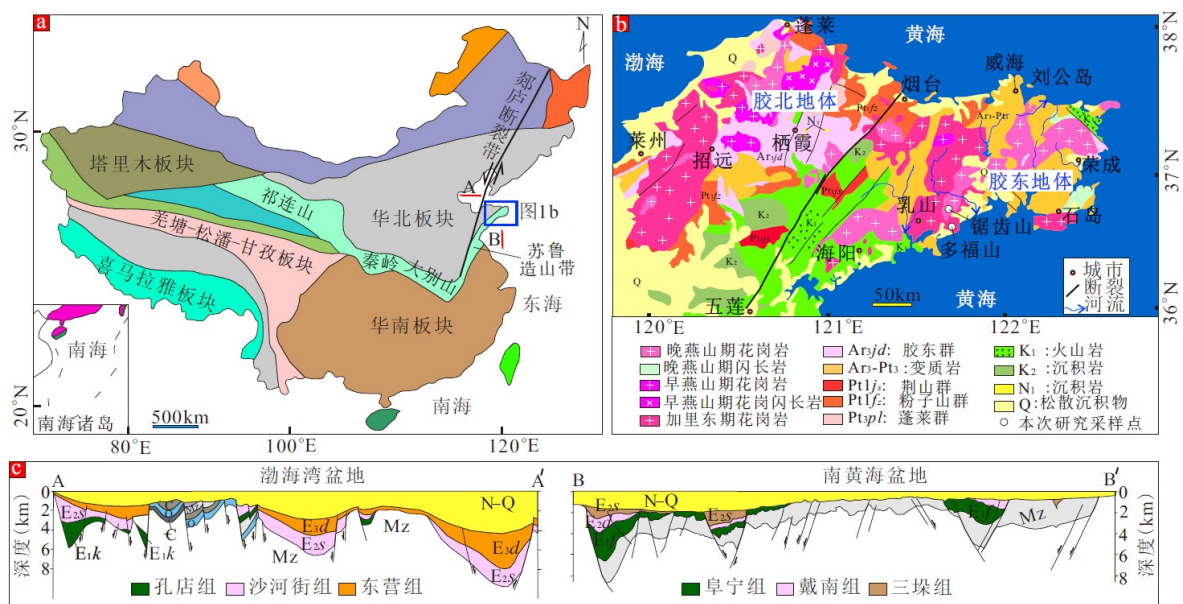
43

44 秦岭-大别-苏鲁造山带是华北克拉通与华南板块在中三叠世发生陆-陆碰撞形成的陆内造山  
45 带(Wu and Zheng, 2013; Li et al., 2019, 图 1a)。它不仅是世界上出露规模最大、保存最好的超高  
46 压变质地体之一，而且也是陆-陆碰撞之后在超高压岩石折返和剥露过程中岩浆活动最为强烈  
47 的地区之一(Zheng et al., 2008; 朱日祥等, 2020)。因此是研究陆-陆碰撞引起岩体剥露过程的理  
48 想靶区(Hu et al., 2006; Wu et al., 2016; Ding et al., 2021)。对其剥露(构造过程、地表侵蚀等作用  
49 造成地表或地下某一点物质的垂直移离)时间的限定，有助于理解中国中东部陆内造山带的演  
50 化过程及其动力学机制(周祖翼, 2015)。前人曾对秦岭、大别山和苏鲁造山带中、新生代期间  
51 的剥露历史开展了大量研究，集中在其西部(陈安定等, 2004; 胡圣标等, 2005; Hu et al., 2006; Liu  
52 et al., 2009; Siebel et al., 2009; Zhang et al., 2020; Ding et al., 2021)和东段的北部(Wu et al., 2016,  
53 2017; Zhao et al., 2018)。而苏鲁造山带南部的数据相对匮乏，因此整个苏鲁造山带在新生代何  
54 时开始整体剥露一直没有得到很好的厘定，同时在空间上苏鲁造山带东段南北的剥露时间是否  
55 同步也尚不可知。

56 磷灰石(U-Th)/He 年龄体系具有已知最低的放射性同位素封闭温度(70°C)(Jolivet et al.,  
57 2010; Shen et al., 2016; 张炜斌等, 2016; Yang et al., 2016; Wu et al., 2021)，近年来已被广泛应用  
58 于造山带剥露研究(Wu et al., 2017, 2020; Liu-Zeng et al., 2018; 林旭和刘静, 2019; Yu et al., 2019;  
59 Ge et al., 2020; Cao et al., 2021; Ding et al., 2021)。因而，为了解答上述问题，我们对苏鲁造山  
60 带东段胶东半岛南部的锯齿山和多福山开展了基岩磷灰石(U-Th)/He 年龄分析，并与周缘已有  
61 的低温热年代学结果进行了对比分析，获得了区域内新生代早期两阶段剥露事件新证据，这可  
62 为更好的认识中国东部盆山分布格局重建提供重要参考。

## 631 地质背景

64 苏鲁造山带位于中国中东部，宽约 180 km，长约 750 km，整体呈北东-南西向展布，通常  
 65 被认为是大别造山带的延伸，但被北东向的郯庐断裂带大幅度左旋错断(许立青等，2016; Wu e  
 66 t al., 2016)。苏鲁造山带是中三叠世华北克拉通与华南板块之间的陆陆碰撞造山的产物(Li et al.,  
 67 2019)，也是世界范围内出露最好的超高压变质地体之一，已成为研究陆-陆碰撞造山过程的天  
 68 然实验室(Liu et al., 2009; Wu and Zheng, 2013; Wu et al., 2017)。苏鲁造山带东段现今地表出露  
 69 的岩石类型以新元古代花岗片麻岩和中生代岩浆岩为主(Zheng, 2008)。苏鲁造山带最东端即胶  
 70 东半岛，该区以五莲-烟台断裂为界(图 1b)，在构造上可分为胶北地体和胶东地体(山东区域地  
 71 质志, 1991)。其中胶北地体具有华北克拉通的属性，而胶东地体具有苏鲁超高压的属性，中生  
 72 代岩浆广泛侵入其中。前人的锆石 U-Pb 年龄(Tang et al., 2008; Yang and Santosh, 2014)表明该区  
 73 的中生代岩浆岩主要形成于晚三叠纪(225-205 Ma)，晚侏罗纪(160-150 Ma)和早白垩纪(130-110  
 74 Ma)。南黄海盆地(Zhu et al., 2020)和渤海湾盆地(Tan et al., 2018; Sun et al., 2020)是位于苏鲁造  
 75 山带南北两侧的中-新生代沉积盆地，保存其内的碎屑沉积地层出现角度不整合指示区域内在  
 76 新生代期间发生了两期构造事件(图 1c)，分别发生在始新世和渐新世。



77

78 图 1 苏鲁造山带位置图(a)，(b)胶东半岛地质简图(修改自中国 1:250 万地质图)；(c) A-A'和 B-B'  
 79 代表渤海湾盆地和南黄海盆地地震反射剖面

80 Fig. 1 Location map of Sulu orogenic belt, (b) Geological map of Jiaodong Peninsula (Modified from  
 81 China 1:2.5 million geological map); (c) A-A' and B-B' represent seismic reflection profiles of the  
 82 Bohai Bay Basin and the South Yellow Sea Basin

83

### 842.1 样品采集

85 为了更好约束胶东地体南部的剥蚀历史, 本文的磷灰石(U-Th)/He 热年代学研究采用年龄-高  
86程法来进行样品采集。我们在胶东地体南部的锯齿山和多福山共采集年代学样品 8 件。其中样  
87品 D1-D3 采自多福山中粗粒闪长岩(锆石 U-Pb 年龄 161 Ma, 郭敬辉等, 2005, 表 1); 样品 L1-L5  
88采自锯齿山中粗粒二长黑云母花岗岩(锆石 U-Pb 年龄 119.6-114.2 Ma, 李增达等, 2018)。多福山  
89样品采集高程为 126-350m, 样品采集的高差为 100 m; 锯齿山样品采集高程为 65-383 m, 样品  
90采集高差为 50-100 m, 采样点可见图 2。

91

表 1 采样位置、高程、岩性数据表

92

Table 1 Sample location, elevation, petrology

样品号	海拔(m)	经度	纬度	岩性
D1	350	36°53'03"	121°43'12"	闪长岩
D2	253	36°52'59"	121°43'06"	闪长岩
D3	126	36°52'51"	121°43'02"	闪长岩
L1	383	36°56'14"	121°40'09"	花岗岩
L2	293	36°55'53"	121°40'08"	花岗岩
L3	179	36°55'47"	121°39'53"	花岗岩
L4	123	36°55'32"	121°39'40"	花岗岩
L5	65	36°55'22"	121°39'20"	花岗岩



93 121°31'E 121°38'E 121°45'E

94 图 2 多福山和锯齿山地质图(修改自乳山 1:20 万区域地质图)和样品采集点分布图

95 Fig. 2 Geological map of Duofu and Juchi Mountains(Modified from Rushan 1:200,000 regional

96 geological map) and distribution map of sample collection points

97

98 **2.2 实验方法**

99 磷灰石(U-Th)/He 测试工作在中国科学院地质与地球物理研究所  $^{40}\text{Ar}/^{39}\text{Ar}$  和(U-Th)/He 年代

100 学实验室完成。主要实验流程是, 首先经过标准的岩石破碎和重液分离程序, 在显微镜下优先

101 选择宽度超过  $60\ \mu\text{m}$  的晶粒, 确保颗粒中没有可见的包裹体和内部裂缝, 对 2-5 颗自形磷灰石

102 进行精确测量, 以实现  $\alpha$  校准因子( $F_c$ )的计算。然后将每个颗粒包裹在  $1\text{mm}\times 1\text{mm}$  铂(Pt)胶囊

103 中, 并将其装入无氧铜盘中。使用 Alphachron MK II (Australian Scientific Instrument Pty

104 Limited)仪器进行氦(He)含量提取。之后将铂包裹磷灰石颗粒转移到 Savillex PFA 瓶中, 加入已

105 知浓度的  $^{230}\text{Th}$  -  $^{235}\text{U}$  溶液。所有加标溶液在 Thermo Fisher X-II 电感耦合等离子体质谱(ICP-MS)

106 上测量。最后年龄计算由基于 Java 程序的 Helioplot 软件实现(Vermeesch, 2010), 并按照

107 Gautheron 等(2009)的程序对  $\alpha$  离子射出效应( $F_e$ )进行校正。MK-1 磷灰石作为参考标准来验证

108 实验分析精度(Wu et al., 2019)。具体实验流程可参考 Wu et al. (2016, 2019)。

109 磷灰石的(U-Th)/He 测试结果不仅可以提供样品的热年代学年龄值, 通过热历史模拟还可

110 以反演样品经历的热演化史。因此, 本文利用 HeFTy 软件(v1. 9. 3, Ketcham, 2005) 对样品进行

111热历史反演，主要过程是：1) 采用辐射损伤累积和退火模型(RDAAM) (Flowers et al., 2009)；2)  
 112反演时设置 AHe 封闭温度为 70°C，地表温度为 20°C，初始冷却温度范围在 200°C-140°C，输  
 113入所有测量 AHe 年龄的加权平均值，晶粒半径(Rs)，铀(U)、钍(Th)；3) 每个样品颗粒模拟过  
 114程一直进行到获得 100 次以上的“好”的拟合路线(拟合度(GOF)≥0.5)为止。

115

1163 实验结果

1173.1 单颗粒年龄结果

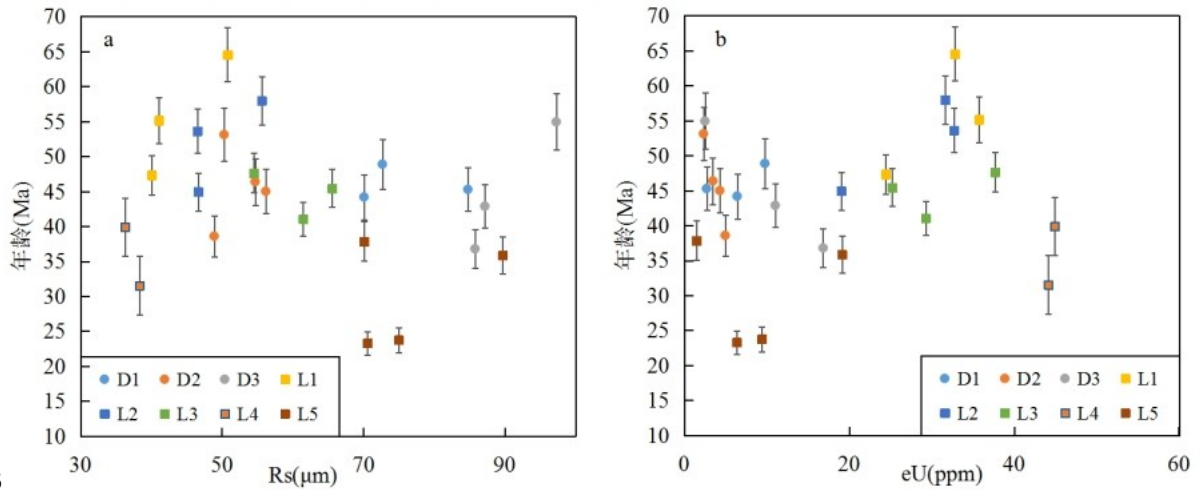
118 本次研究使用的磷灰石(U-Th)/He 数据如表 2 所示。多福山样品 D1 的(U-Th)/He 年龄为  
 11948.9±3.6-44.2±3.2 Ma，平均年龄为 45.9±3.8 Ma。样品 D2 的年龄为 53.1±3.8-38.6±2.9 Ma，平  
 120均年龄为 44.8±3.3 Ma。样品 D3 的年龄为 54.9±4.0-36.8±2.7 Ma，平均年龄为 42.6±3.7 Ma。锯  
 121齿山样品 L1 的(U-Th)/He 年龄为 64.5±3.8-47.3±2.8 Ma，平均年龄为 54.0±3.7 Ma。样品 L2 的年  
 122龄为 57.9±3.4-44.9±2.7 Ma，平均年龄为 51.0±3.5 Ma。样品 L3 的年龄为 47.6±2.8-41.1±2.4

123Ma，平均年龄为 44.4±3.1 Ma。样品 L4 的年龄为 39.9±2.4-31.5±1.9 Ma，平均年龄为 34.7±3.0  
 124Ma。样品 L5 的年龄为 37.9±2.8-23.3±1.7 Ma，平均年龄为 27.3±2.0 Ma。此外，AHe 年龄的准  
 125确解释必须考虑晶粒尺寸(半径, Rs)和有效 U 浓度( $eU = U + 0.235 \times Th$ )的影响，因为这两个参数  
 126对 He 扩散有不可忽视的影响(Reiners and Farley, 2001)，我们通过 AHe 年龄与 Rs 大小(图 3a)和  
 127eU(图 3b)二维散点图来判别是否具有相关性。结果表明，无论是多福山还是锯齿山的样品，  
 128其 AHe 年龄与 Rs 和 eU 不存在正相关关系，说明晶粒尺寸或辐射损伤并未对 AHe 年龄产生影  
 129响(Reiners and Farley, 2001; Shuster et al., 2006)。

样品号	质量 (μg)	半径 (μm)	U (ppm)	Th (ppm)	eU (ppm)	初始年龄 (Ma)	FT (Ma)	年龄 (Ma)	年龄 (Ma)	
D1-A1	8.31	70.1	6	1.8	6.4	35.57	1.89	0.805	44.19	3.22
D1-A2	15.12	84.8	2.3	2	2.7	37.76	1.76	0.834	45.28	3.09
D1-A3	9.4	72.7	9.3	2	9.8	39.68	2.12	0.812	48.87	3.58
D2-A1	3.31	50.3	2	1.2	2.3	38.77	1.98	0.73	53.11	3.8
D2-A2	2.74	48.9	3.8	3	3	27.78	1.8	0.72	38.58	2.94
D2-A3	4.02	54.7	3	2	3.5	34.78	1.82	0.75	46.37	3.36
D2-A4	4.58	56.2	3.8	2.2	4.3	34.02	1.72	0.756	45	3.2
平均年龄									44.8	3.3
D3-A2	22.29	97.3	2.4	0.5	2.5	47.07	2.53	0.857	54.92	4.03
D3-A3	17.89	87.2	10.3	2.5	12.5	36.92	1.842		42.87	3.13

130 表 2 多福山和锯齿山垂直剖面磷灰石(U-Th)/He 年龄结果  
 131 Table 2 (U-Th)/He analytical results for samples in the vertical transect in the Dufu and Juchi Shan

样品号	质量 (μg)	半径 (μm)	U (ppm)	Th (ppm)	eU (ppm)	初始年龄 (Ma)	FT (Ma)	年龄 (Ma)	年龄 (Ma)	
平均年龄									42.6	3.7
L1-A1	1.83	41.1	14.2	91.7	35.7	35.84	1.16	0.65	55.14	3.28
L1-A4	3.49	50.8	13.3	83.1	32.8	46.02	1.49	0.713	64.54	3.84
L1-A5	1.54	40	10.3	60.2	24.5	30.52	1.01	0.645	47.32	2.84
平均年龄									54.0	3.7
L2-A1	2.58	46.6	8	46.9	19	31	1.02	0.69	44.93	2.69
L2-A2	2.54	46.5	12.7	85.2	32.7	36.9	1.19	0.688	53.63	3.19
L2-A4	4.2	55.6	12.6	80.8	31.6	42.65	1.37	0.736	57.95	3.44
平均年龄									51.0	3.5
L3-A1	5.99	61.5	11.6	75.2	29.3	31.17	1	0.759	41.07	2.44
L3-A2	7.54	65.6	10.9	61.1	25.2	35.21	1.15	0.775	45.43	2.71
L3-A3	4.06	54.5	16.1	91.6	37.7	34.86	1.13	0.732	47.62	2.84
平均年龄									44.4	3.1
L4-A1	1.52	38.3	17.1	115.3	44.2	19.76	0.65	0.627	31.52	1.89
L4-A2	1.31	36.3	18	114.6	44.9	24.33	0.79	0.61	39.89	2.38
平均年龄									34.7	3.0
L5-A1	9.33	70.6	5.8	2.6	6.4	18.74	0.96	0.805	23.28	1.67
L5-A2	7.93	70.1	1.4	0.5	1.5	30.44	1.65	0.804	37.86	2.79
L5-A3	10.86	75	9.2	1.2	9.4	19.42	1.05	0.818	23.74	1.75
L5-A4	16.89	89.7	18.5	2.6	19.1	30.35	1.64	0.847	35.83	2.64
平均年龄									27.3	2.0



133

134 图 3 磷灰石 He 年龄和颗粒半径(Rs)(a)、有效铀浓度(eU)(b)二维散点图

135 Fig. 3 Scatter diagram of apatite He age, grain radius (Rs)(a) and effective uranium concentration (Eu)

136 (b)

137

### 138 3.2 年龄高程剖面

139 本次所有样品测试年龄远小于其岩体结晶基底锆石 U-Pb 年龄，表明磷灰石(U-Th)/He 年龄

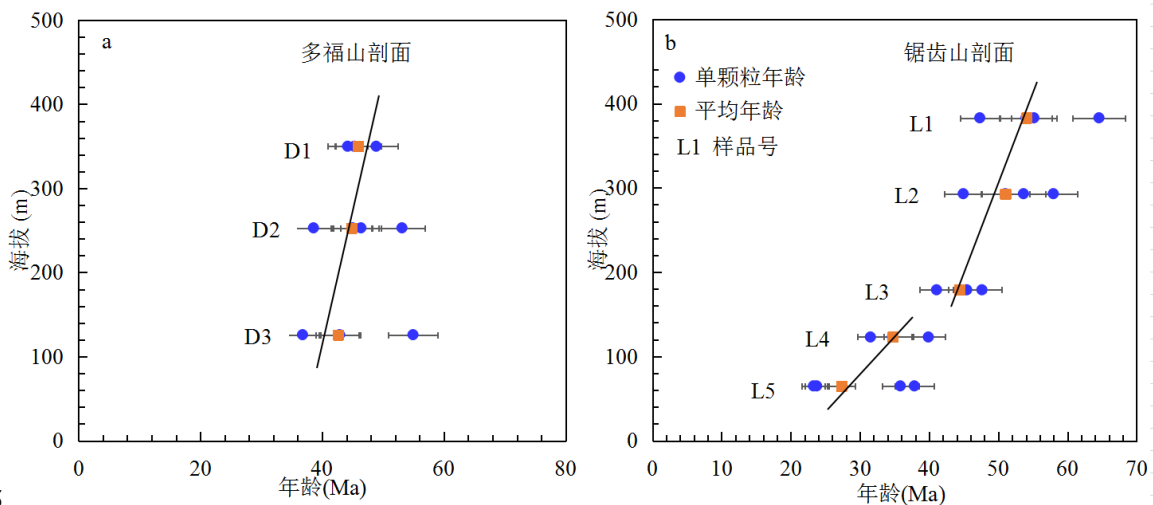
140 是后期因剥露去顶通过部分保存带(PRZ)的冷却年龄。多福山剖面底部 D3 样品平均年龄为

141  $42.6 \pm 3.7$  Ma(图 4a)，向上 D1 样品的平均年龄递增到  $45.9 \pm 3.8$  Ma，锯齿山底部样品 L5 的平均

142 年龄为  $27.3 \pm 2.0$  Ma(图 4b)，向上样品 L4 的平均年龄为  $34.7 \pm 3.0$  Ma；样品 L3 的平均年龄为

143  $44.4 \pm 3.1$  Ma，向上样品 L1 的平均年龄为  $54.0 \pm 3.7$  Ma。总体来看，两个剖面的实测磷灰石(U-

144 Th)/He 年龄符合各自的年龄-高程图，即年龄自底部向上依次递增。



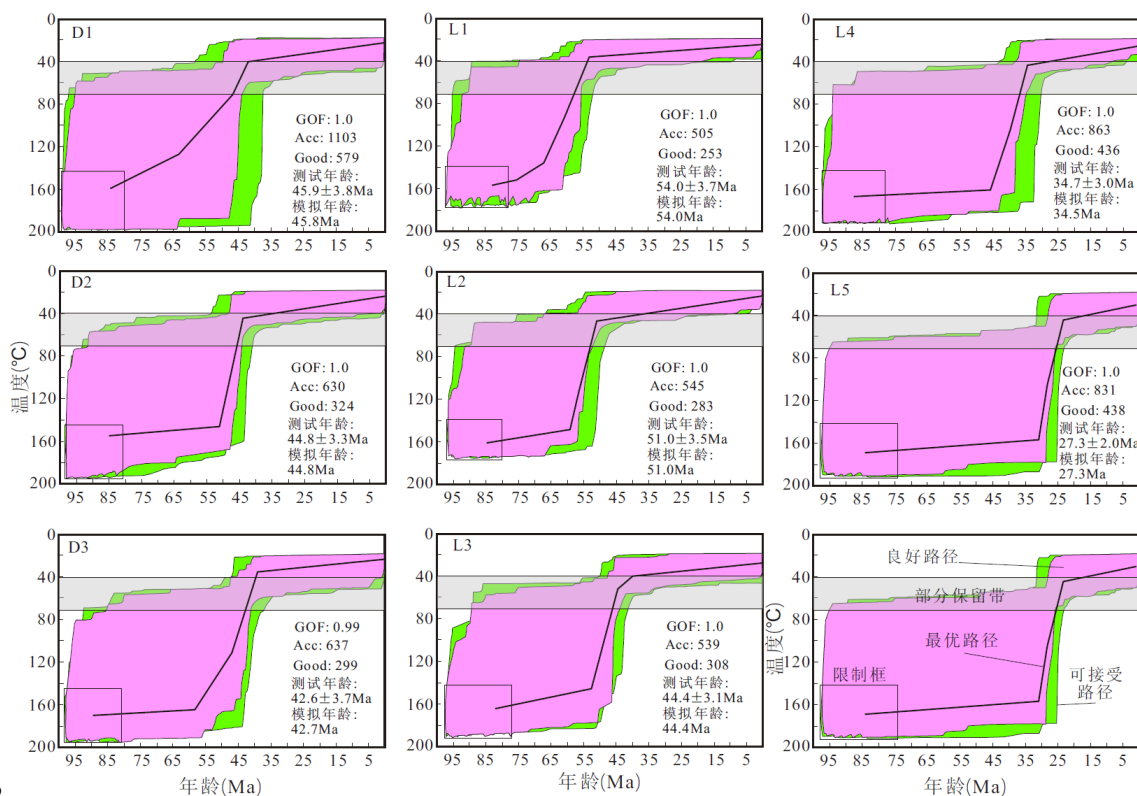
145

146 图 4 年龄-高程关系图，(a)多福山剖面；(b)锯齿山剖面

147 Fig. 4 Age-elevation relationship diagram, (a) Duofu Mountain profile; (b) Juchi Mountain profile

### 148 3.3 热历史反演结果

149 图5展示了多福山3个和锯齿山5个样品的单颗粒模拟结果，每个样品均显示了单一的冷150却历史，多福山样品在45.8-42.7 Ma，锯齿山上部3个样品在54.0-44.4 Ma，底部2个样品在15134.7-27.3 Ma快速通过部分保留带。2个剖面的单颗粒模拟年龄结果与实测数据结果一致。



152

153 图5 多福山(D1-D3)和锯齿山(L1-L5)单颗粒磷灰石(U-Th)/He 年龄模拟结果

154 Fig. 5 The modeled thermal histories of samples from Duofu (D1-D3) and Juchi (L1-L5) Mountains.

155

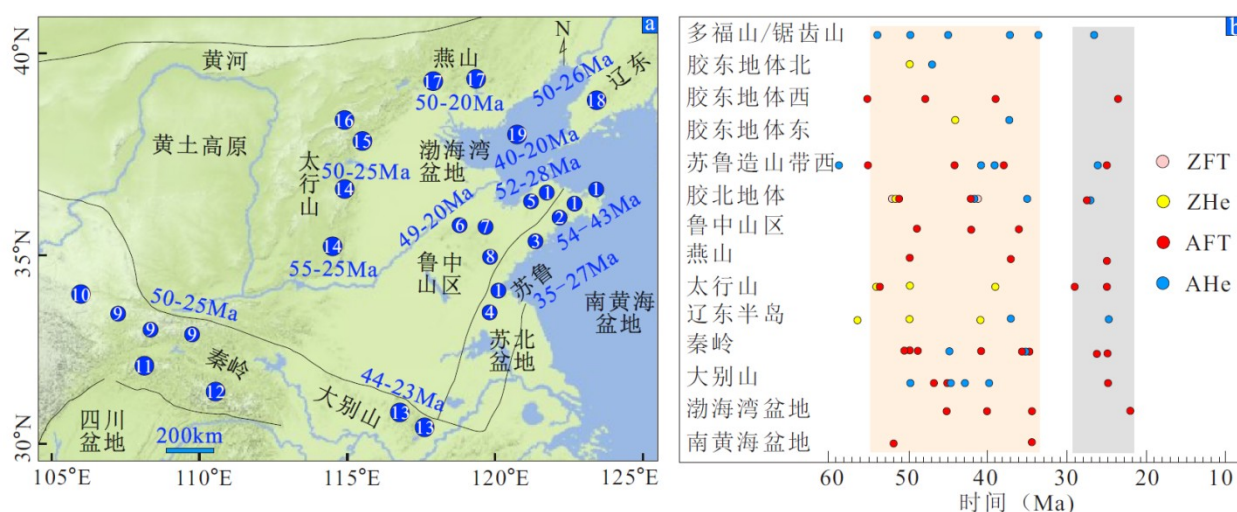
## 1564 讨论

### 1574.1 苏鲁造山带东段新生代两阶段剥露过程

158 年龄-高程对应关系和热历史模拟结果表明，多福山和锯齿山在早-中始新世(54-43 Ma)和  
 159渐新世(35-27 Ma)出现两阶段剥露过程。锆石和磷灰石(U-Th)/He 年龄，揭示胶东地体北部烟台、  
 160威海附近的岩体在 50-47 Ma 发生冷却抬升(Wu et al., 2016, 2017, 图 6a)。磷灰石 FT 年龄表明海  
 161阳北部和乳山北部岩体在 48-24 Ma 和 39 Ma 出现剥露过程(Zhao et al., 2018)。胶东地体东部荣  
 162成和石岛附近的岩体在 44 Ma(Wu et al., 2016)和 39 Ma 发生剥露(Siebel et al., 2009)。青岛附近  
 163的崂山岩体在 55 Ma 发生剥露(胡圣标等, 2005)。因而，苏鲁造山带东段在始新世和渐新世经历  
 164了广泛的剥露过程，其南北剥露时间具有时空同步性。磷灰石 FT 年龄记录了苏鲁造山带西段  
 165东海附近岩体在新生代早-中始新世(55-44 Ma)和渐新世(38-25 Ma)发生剥露(陈安定等, 2004;  
 166Liu et al., 2009)。Wu 等(2016)对日照和东海附近中生代花岗岩岩体开展磷灰石(U-Th)/He 年龄

167分析, 表明新生代剥露事件分别发生在 59-41 Ma 和 39-26 Ma。这说明苏鲁造山带在这个时间  
168内出现整体抬升过程。

169 从更大的范围来看, 锆石和磷灰石低温热年代学结果(Deng et al., 2015; Wu et al., 2016; Liu  
170et al., 2017; Sun et al., 2017; Zhao et al., 2017), 指示了胶北地体新生代剥露主要发生在早-中始  
171新世(52-41 Ma)和渐新世(35-28 Ma)。鲁中山区在 49-42 Ma 和 36-20 Ma 发生剥露(唐智博等,  
1722011; 许立青等, 2016; 李理等, 2018)。碎屑磷灰石 FT 年龄揭示渤海湾盆地的沉积地层在 45-40  
173Ma 和 34-20 Ma 经历了挤压抬升过程(Chang et al., 2018; Xu et al., 2020), 同时其西部的太行山  
174在 55-40 Ma 和 30-25 Ma 发生剥露(Cao et al., 2015; Chang et al., 2019; Wu et al., 2020; Clinkscales  
175et al., 2021; Su et al., 2021; Zhang et al., 2021)。碎屑磷灰石 FT 年龄记录了南黄海盆地在 52 Ma  
176和 38 Ma 发生地层抬升剥蚀事件(庞玉茂等, 2018; Pang et al., 2019)。同期构造事件也发生在燕  
177山(吴中海和吴珍汉, 2003)、辽东半岛(Wang et al., 2018)、秦岭(Liu et al., 2013; Wang et al., 2013;  
178Chen et al., 2015; Yang et al., 2017; Zhang et al., 2020)和大别山(Grimmer et al., 2002; Reiners et al.,  
1792003; Hu et al., 2006; 周祖翼, 2015; Ding et al., 2021)。这说明在新生代早期中国东部普遍经历了  
180两阶段抬升过程(图 6b)。



181

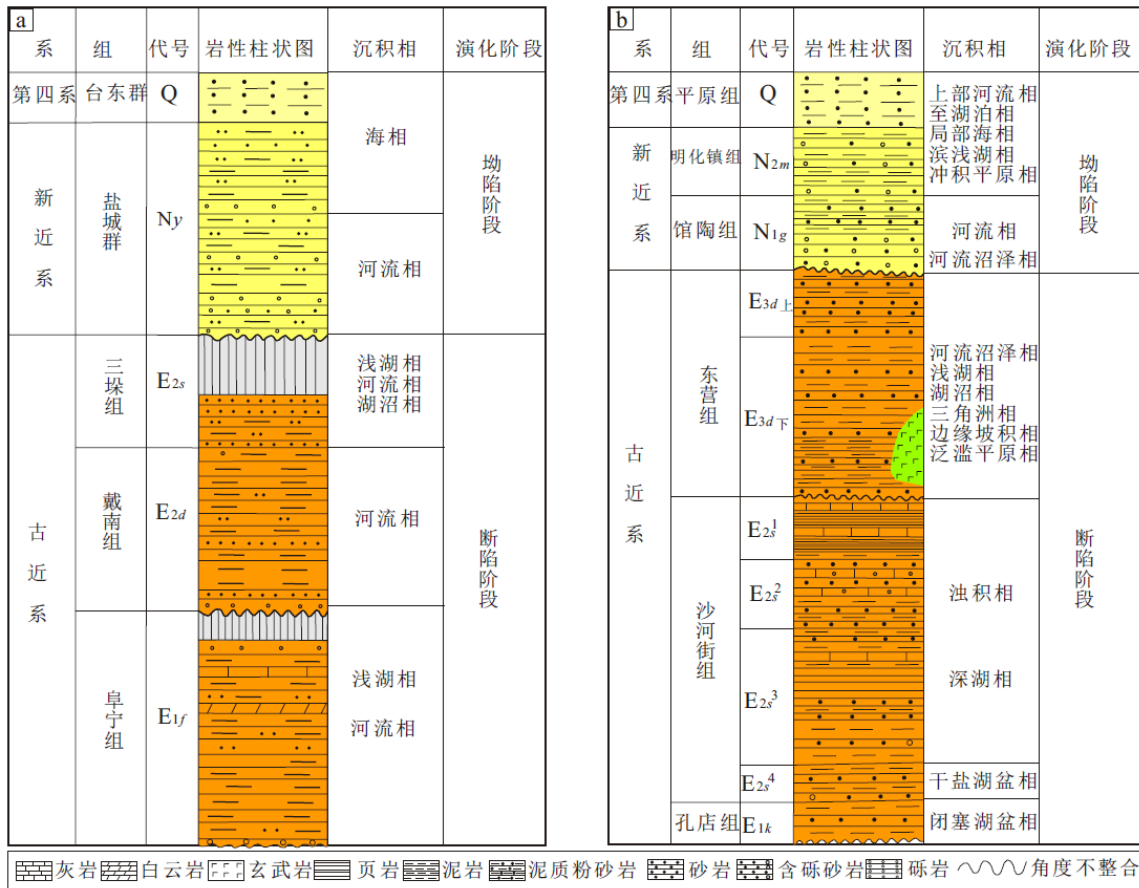
182图 6 苏鲁造山带及其邻近区域早新生代构造隆升事件位置分布图(a)和时间汇总图(b), 图 a 中  
183数字代表研究位置: (1) Wu et al.(2016); (2) Zhao et al.(2018); (3) 胡圣标等(2005); (4) Liu et al.  
184(2009); (5) Liu et al.(2009); (6)唐智博等(2011); (7)李理等(2018); (8) 许立青等(2016); (9) Liu et al.  
185(2013); (10) Wang et al.(2013); (11) Zhang et al.(2020); (12)Yang et al.(2017); (13) Hu et al.(2006);  
186(14) Cao et al.(2015), Chang et al.(2019), Zhang et al.(2021); (15) Wu et al.(2020); (16) Clinkscales et  
187al.(2021); (17)吴中海和吴珍汉(2003); (18) Wang et al.(2018); (19) Chang et al.(2018), Xu et al.  
188(2020)

189Fig. 6 Distribution map of available exhumation ages (a) and time summary diagram (b) of early

190 Cenozoic tectonic uplift events in the Sulu orogenic belt and adjacent areas. The numbers in blue  
191 circles indicate the position of referenced works.

#### 192 4.2 苏鲁造山带新生代隆升与邻区盆地的耦合关系

193 造山带隆升(地表相对于大地水准面或平均海平面的位移)产生的碎屑沉积物被搬运至邻近  
194 盆地, 因而这些保存于沉积盆地的碎屑沉积物的沉积学和地层变形信息可用于恢复造山带的隆  
195 升过程(Chang et al., 2018; 林旭和刘静, 2019; Zhu et al., 2020)。碎屑锆石 U-Pb 年龄和重矿物物  
196 源示踪结果表明, 南黄海盆地北部始新统地层(55-38 Ma)的碎屑物质主要来自胶东地体(Zhu et  
197 al., 2020)。碎屑锆石 U-Pb 年龄、重矿物和砂岩组分分析, 说明苏北盆地(张妮, 2012)和南黄海  
198 盆地南部(Zhu et al., 2020)始新统地层的物质主要来自苏鲁造山带西段。结合苏北盆地(舒良树  
199 等, 2005; 邱燕等, 2016)和南黄海盆地(陈亮等, 2008)的地层在 55-50 Ma 和 38-25 Ma 分别出现角  
200 度不整合, 并缺失部分地层(邱燕等, 2016, 图 7a), 说明此时区域发生构造变形事件。物源示踪  
201 结果结合地层的沉积时代表明, 胶北地体(Sun et al., 2020)、鲁中山区(Liu et al., 2020)、太行山  
202 (Chen et al., 2020)和燕山(Tan et al., 2018; Liu et al., 2019)在早-中始新世和渐新世向渤海湾盆地  
203 提供碎屑物质, 同时在盆地内沉积地层出现角度不整合、底砾岩(邱燕等, 2016; Chang et al.,  
204 2018)(图 7a), 说明这些碎屑物质的输入可主要归结为造山带的隆升剥蚀。所以, 从盆地沉积  
205 学的角度也佐证了苏鲁造山带及其邻近区域在早-中始新世和晚渐新世发生构造变形事件。



206

207图 7 渤海湾盆地和南黄海盆地沉积柱状图(修改自邱燕等, 2016)

208Fig. 7 Synthetic sedimentary columns of the Bohai Bay Basin and South Yellow Sea Basin (Modified from Qiu et al., 2016)

209

210

211 苏鲁造山带早-中始新世和晚渐新世剥露过程与周缘板块活动时间相吻合。Northrup 等

212(1995)认为太平洋板块向西俯冲在中国东部造山带、盆地构造演化中起主导作用。早-中始新世

213(50-43 Ma)西太平洋板块以 NNW 向俯冲到欧亚大陆下部(Tarduno, 2007; Yin, 2010; Li et al.,

2142015; Zhu and Xu et al., 2019), 俯冲速率由晚白垩纪的 140-120 mm/a 下降到 40-30

215mm/a(Northrup et al., 1995; 包汉勇等, 2008; Liang and Wang, 2019), 此时西太平洋板块发生俯冲

216回撤, 中国东部处于伸展拉张环境, 在此构造背景下出现软流圈上涌、岩石圈拆沉(Yin, 2010;

217Li et al., 2015), 驱动苏鲁造山带发生构造抬升(Hu et al., 2006; Wu et al., 2016; Ding et al.,

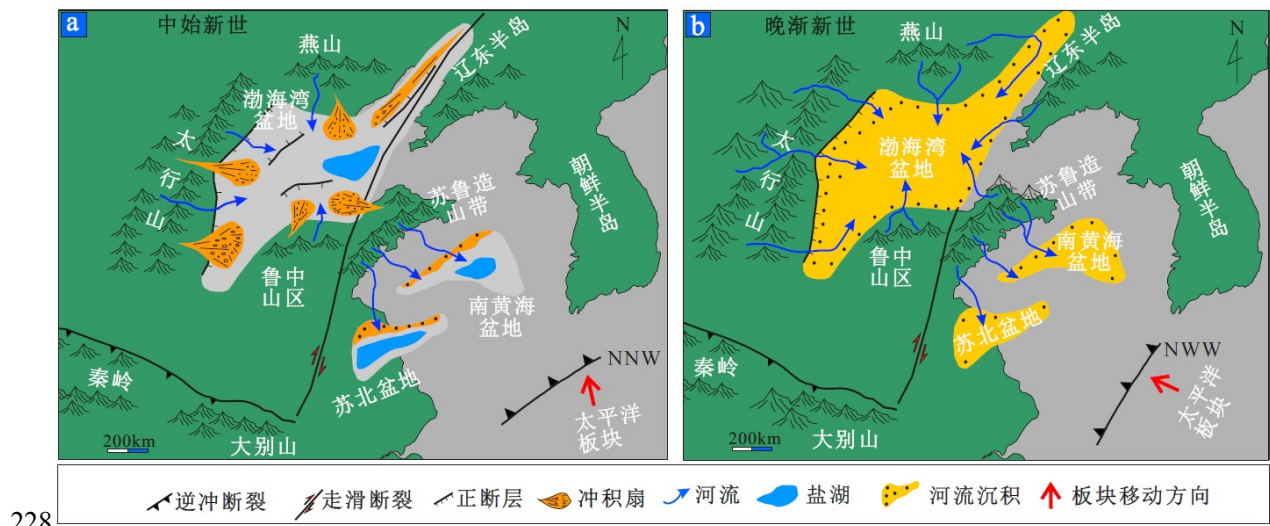
2182021), 其周围出现南黄海、渤海湾等大型断陷盆地(Ren et al., 2002; Su et al., 2014a; Suo et al.,

2192014), 中国东部造山带与盆地的这一差异升降导致盆山地貌开始分异。受盆地断陷过程的影

220响, 这些沉积中心此时彼此分隔, 未形成统一的沉积分布区(图 1c, 图 6a)。进入晚渐新世(32-

22123 Ma), 太平洋板块向欧亚大陆俯冲的速率维持在 95-70 mm/a(Northrup et al., 1995; 包汉勇等,

2222008; Liang and Wang, 2019), 俯冲方向转变为 NWW(Li et al., 2015), 中国东部伸展拉张环境逐  
 223渐减弱, 开始以构造挤压背景为主(Ren et al., 2002; Su et al., 2014b), 这促使苏鲁造山带、鲁中  
 224山区、太行山和燕山山脉内部基岩遭受新一期剥露, 邻近的南黄海、渤海湾等盆地发生地层缺  
 225失或构造变形, 上述造山带隆升-剥露产生的碎屑物质进入南黄海盆地和渤海湾盆地后, 导致  
 226后者开始进入坳陷演化阶段, 盆山耦合关系进一步加强, 从而奠定了中国东部盆-山地貌分布  
 227格局的雏形(图 6b)。



229 图 7 早新生代中国东部盆山分布复原图  
 230 Fig. 7 Palaeogeographic maps showing the distribution of basins and mountains in eastern China  
 231 during the early Cenozoic. Note that maps are drawn using a present-day coastline.

2326 结论

233 本文利用磷灰石(U-Th)/He 热年代学方法约束苏鲁造山带东段南部的多福山和锯齿山的剥  
 234露时间, 得到如下结论:

235(1) 年龄-高程对应关系和热历史模拟结果表明多福山和锯齿山在早-中始新世(54-43 Ma)和渐新  
 236世(35-27 Ma)发生剥露。苏鲁造山带东段的南、北部在新生代的剥露时间基本一致;

237(2) 综合苏鲁造山带西段的低温热年代学, 邻近南黄海盆地和渤海湾盆地沉积地层出现角度不  
 238整合, 说明苏鲁造山带在早-中始新世和晚渐新世发生阶段性整体剥露。

239(3) 苏鲁造山带及其邻近地区在新生代早期的剥露过程, 主要受控于西太平洋板块向欧亚大陆  
 240俯冲的影响, 自新生代早期以来至少存在两期显著的盆山差异升降过程, 从而奠定中国东部盆  
 241山分布格局。

242

243致谢: 衷心感谢两位审稿人的修改建议以及对文稿的仔细修改。

244参考文献:

245 Bao, H. Y., Guo, Zh. F., Zhang, L. L., et al. 2013. Tectonic dynamics of eastern China since the  
246 formation of the Pacific plate. *Advances in Earth Science*, 28(3), 337-346 (in Chinese with  
247 English abstract).

248 Cao, X., Li, S., Xu, L., et al. 2015. Mesozoic-Cenozoic evolution and mechanism of tectonic  
249 geomorphology in the central North China Block: constraint from apatite fission track  
250 thermochronology. *Journal of Asian Earth Sciences*, 114, 41-53.  
251 <https://doi:10.1016/j.jseaes.2015.03.041>.

252 Cao, K., Leloup, P. H., Wang, G., et al. 2021. Thrusting, exhumation, and basin fill on the western  
253 margin of the South China block during the India-Asia collision. *GSA Bulletin*, 133(1-2), 74-  
254 90. <https://doi:10.1130/B35349.1>.

255 Clinkscales, C., Kapp, P., Thomson, S., et al. 2021. Regional Exhumation and Tectonic History of the  
256 Shanxi Rift and Taihangshan, North China. *Tectonics*, in  
257 press. <https://doi.org/10.1029/2020TC006416>.

258 Chang, J., Qiu, N., Zhao, X., et al. 2018. Mesozoic and Cenozoic tectono-thermal reconstruction of  
259 the western Bohai Bay Basin (East China) with implications for hydrocarbon generation and  
260 migration. *Journal of Asian Earth Sciences*, 160, 380-395.  
261 <https://doi:10.1016/j.jseaes.2017.09.008>.

262 Chang, J., Qiu, N., Liu, S., et al. 2019. Post-Triassic multiple exhumation of the Taihang Mountains  
263 revealed via low-T thermochronology: implications for the paleo-geomorphologic  
264 reconstruction of the North China Craton. *Gondwana Research*, 68, 34-49. <https://doi:10.1016/j.gr.2018.11.007>.

266 Chen, A. D., Guo, T. L., Wan, J. L. 2004. Study on the tectonic uplift of the peripheral upheaval in  
267 Jiangsu and Anhui by using fission track and isotopes dating methods. *Geotectonica et  
268 Metallogenia*, 28(4), 379-387 (in Chinese with English abstract).

269 Chen, L., Liu, Zh. H., Jin, Q. H. et al. 2008. Meso-Cenozoic tectonic evolution of the east depression  
270 of North Yellow Sea. *Geotectonica et Metallogenia*, 32(18), 308-316 (in Chinese with English  
271 abstract).

272 Chen, H., Hu, J., Wu, G., et al. 2015. Apatite fission-track thermochronological constraints on the  
273 pattern of late Mesozoic-Cenozoic uplift and exhumation of the Qinling Orogen, central  
274 China. *Journal of Asian Earth Sciences*, 114, 649-673.  
275 <https://doi:10.1016/j.jseaes.2014.10.004>.

276 Chen, H., Zhu, X., Wood, L. J., et al. 2020. Evolution of drainage, sediment-flux and fluvio-deltaic  
277 sedimentary systems response in hanging wall depocentres in evolving non-marine rift basins:  
278 Paleogene of Raoyang Sag, Bohai Bay Basin, China. *Basin Research*, 32(1), 116-145.  
279 <https://doi:10.1111/bre.12371>.

280 China Geological Survey. 2004. Geological map of the People's Republic of China (1:2.5 million).  
281 Beijing: China map publishing house: 1. (in Chinese)

282 Ding, R., Chang, Y., Min, K., et al. 2021. Post-orogenic topographic evolution of the Dabie orogen,  
283 Eastern China: Insights from apatite and zircon (U-Th)/He  
284 thermochronology. *Geomorphology*, 374, 107487. <https://doi:10.1016/j.geomorph.2020.107487>.

286 Deng, B., Liu, S. G., Li, Z. W., et al. 2013. Differential exhumation at eastern margin of the Tibetan  
287 Plateau, from apatite fission-track thermochronology. *Tectonophysics*, 591, 98-115.

288 <https://doi:10.1016/j.tecto.2012.11.012>.

289Deng, J., Wang, C., Bagas, L., et al. 2015. Cretaceous-Cenozoic tectonic history of the Jiaojia Fault  
290 and gold mineralization in the Jiaodong Peninsula, China: constraints from zircon U-Pb, illite  
291 K-Ar, and apatite fission track thermochronometry. *Mineralium Deposita*, 50(8), 987-1006.  
292 <https://doi:10.1007/s00126-015-0584-1>.

293Flowers, R. M., Ketcham, R. A., Shuster, D. L., et al. 2009. Apatite (U-Th)/He thermochronometry  
294 using a radiation damage accumulation and annealing model. *Geochimica et Cosmochimica*  
295 *acta*, 73(8), 2347-2365. <https://doi:10.1016/j.gca.2009.01.015>.

296Gautheron, C., Tassan-Got, L., Barbarand, J., et al. 2009. Effect of alpha-damage annealing on apatite  
297 (U-Th)/He thermochronology. *Chemical Geology*, 266(3-4), 157-170. [https://](https://doi:10.1016/j.chemgeo.2009.06.001)  
298 [doi:10.1016/j.chemgeo.2009.06.001](https://doi:10.1016/j.chemgeo.2009.06.001).

299Ge, Y., Liu-Zeng, J., Zhang, J., et al. 2020. Spatio-temporal variation in rock exhumation linked to  
300 large-scale shear zones in the southeastern Tibetan Plateau. *Science China Earth*  
301 *Sciences*, 63(4), 512-532. <https://doi:10.1007/s11430-019-9567-y>.

302Grimmer, J. C., Jonckheere, R., Enkelmann, E., et al. 2002. Cretaceous-Cenozoic history of the  
303 southern Tan-Lu fault zone: apatite fission-track and structural constraints from the Dabie Shan  
304 (eastern China). *Tectonophysics*, 359(3-4), 225-253. [https://doi:10.1016/s0040-1951\(02\)00513-](https://doi:10.1016/s0040-1951(02)00513-9)  
305 [9](https://doi:10.1016/s0040-1951(02)00513-9).

306Guo, J. H., Chen, F. Kun., Zhang, X. M. et al. 2005. Evolution of syn- to post-collisional magmatism  
307 from north Sulu UHP belt, eastern China: zircon U-Pb geochronology. *Acta Petrologica*  
308 *Sinica*, 21(4), 1281-1301(in Chinese with English abstract).

309Hu, Sh. B., Hao, J., Fu, M. X. et al. 2005. Cenozoic denudation and cooling history of Qinling-Dabie-  
310 Sulu orogens: apatite fission track thermochronology constrains. *Acta Petrologica Sinica*,  
311 21(4), 1167-1173(in Chinese with English abstract).

312Hu, S., Kohn, B. P., Raza, A., et al. 2006. Cretaceous and Cenozoic cooling history across the  
313 ultrahigh pressure Tongbai-Dabie belt, central China, from apatite fission-track  
314 thermochronology. *Tectonophysics*, 420(3-4), 409-429. <https://doi:10.1016/j.tecto.2006.03.027>.

315Jolivet, M., Dominguez, S., Charreau, J., Chen, Y., Li, Y., Wang, Q. 2010. Mesozoic and Cenozoic  
316 tectonic history of the central Chinese Tian Shan: reactivated tectonic structures and active  
317 deformation. *Tectonics*, 29(6), 1-30. <https://doi.org/10.1029/2010TC002712>.

318Ketcham, R. A. 2005. Forward and inverse modeling of low-temperature thermochronometry  
319 data. *Reviews in mineralogy and geochemistry*, 58(1), 275-314.  
320 <https://doi:10.2138/rmg.2005.58.11>.

321Li, L., Zhong, D. L., Chen, X. F. et al. 2018. Characteristics of NW-trending faults and evidence of  
322 fission track in the Luxi Block. *Acta Geologica Sinica*, 92(3), 413-436 (in Chinese with  
323 English abstract).

324Li, Z. D., Yu, X. F., Wang, Q. M. et al. 2018. Petrogenesis of Sanfoshan granite, Jiaodong: Diagenetic  
325 physical and chemical condition, zircon U-Pb geochronology and Sr-Nd isotope constraints.  
326 *Acta Petrologica Sinica*, 34(2), 447-468(in Chinese with English abstract).

327Li, S., Guo, L., Xu, L., et al. 2015. Coupling and transition of Meso-Cenozoic intracontinental  
328 deformation between the Taihang and Qinling Mountains. *Journal of Asian Earth*  
329 *Sciences*, 114, 188-202. <http://dx.doi.org/10.1016/j.jseaes.2015.04.011>.

330Li, S., Suo, Y., Li, X., et al. 2019. Mesozoic tectono-magmatic response in the East Asian ocean-

331 continent connection zone to subduction of the Paleo-Pacific Plate. *Earth-Science*  
332 *Reviews*, 192, 91-137. <https://doi.org/10.1016/j.earscrev.2019.03.003>.

333Liang, J., Wang, H. 2019. Cenozoic tectonic evolution of the East China Sea Shelf Basin and its  
334 coupling relationships with the Pacific Plate subduction. *Journal of Asian Earth Sciences*, 171,  
335 376-387. <https://doi.org/10.1016/j.jseaes.2018.08.030>.

336Lin, X., Liu, J. 2019. A review of mountain-basin coupling of Jiangnan and Dongting basins with their  
337 surrounding mountains. *Seismology and Geology*, 41(2), 499-520(in Chinese with English  
338 abstract).

339Liu, S. S., Weber, U., Glasmacher, U. A., et al. 2009. Fission track analysis and thermotectonic history  
340 of the main borehole of the Chinese Continental Scientific Drilling  
341 project. *Tectonophysics*, 475(2), 318-326. <https://doi.org/10.1016/j.tecto.2009.03.015>.

342Liu, J., Zhang, P., Lease, R. O., et al. 2013. Eocene onset and late Miocene acceleration of Cenozoic  
343 intracontinental extension in the North Qinling range–Weihe graben: Insights from apatite  
344 fission track thermochronology. *Tectonophysics*, 584, 281-296.  
345 <https://doi.org/10.1016/j.tecto.2012.01.025>.

346Liu, X., Fan, H. R., Evans, N. J., et al. 2017. Exhumation history of the Sanshandao Au deposit,  
347 Jiaodong: constraints from structural analysis and (U-Th)/He thermochronology. *Scientific*  
348 *reports*, 7(1), 1-12. <https://doi.org/10.1038/s41598-017-08103-w>.

349Liu, Q., Zhu, X., Zeng, H., et al. 2019. Source-to-sink analysis in an Eocene rifted lacustrine basin  
350 margin of western Shaleitian Uplift area, offshore Bohai Bay Basin, eastern China. *Marine*  
351 *and Petroleum Geology*, 107, 41-58. <https://doi.org/10.1016/j.marpetgeo.2019.05.013>.

352Liu, H., van Loon, A. T., Xu, J., et al. 2020. Relationships between tectonic activity and sedimentary  
353 source-to-sink system parameters in a lacustrine rift basin: A quantitative case study of the  
354 Huanghekou Depression (Bohai Bay Basin, E China). *Basin Research*, 32(4), 587-612. <https://doi.org/10.1111/bre.12374>.

356Liu-Zeng, J., Zhang, J., McPhillips, D., et al. 2018. Multiple episodes of fast exhumation since  
357 Cretaceous in southeast Tibet, revealed by low-temperature thermochronology. *Earth and*  
358 *Planetary Science Letters*, 490, 62-76. <https://doi.org/10.1016/j.epsl.2018.03.011>.

359Northrup, C. J., Royden, L. H., Burchfiel, B. C. 1995. Motion of the Pacific plate relative to Eurasia  
360 and its potential relation to Cenozoic extension along the eastern margin of  
361 Eurasia. *Geology*, 23(8), 719-722.  
362 [https://doi.org/10.1130/0091-7613\(1995\)023<0719:MOTPPR>2.3.CO;2](https://doi.org/10.1130/0091-7613(1995)023<0719:MOTPPR>2.3.CO;2).

363Pang, Y., Guo, X., Han, Z., et al. 2018. Analysis of apatite fission track of strata denudation since Late  
364 Cretaceous in the central uplift of South Yellow Sea. *Earth Science*, 43(6), 1921-1930(in  
365 Chinese with English abstract).

366Pang, Y. M., Guo, X. W., Han, Z. Z., et al. 2019. Mesozoic-Cenozoic denudation and thermal history  
367 in the Central Uplift of the South Yellow Sea basin and the implications for hydrocarbon  
368 systems: Constraints from the CSDP-2 borehole. *Marine and Petroleum Geology*, 99, 355-369.

369Qiu, Y., Wang, L. F., Huang, W. K. 2016. The Mesozoic and Cenozoic Sedimentary Basins in the Sea  
370 Area of China. *Geological Publishing House*, Beijing, 1-233(in Chinese with English abstract).

371Ren, J., Tamaki, K., Li, S., et al. 2002. Late Mesozoic and Cenozoic rifting and its dynamic setting in  
372 Eastern China and adjacent areas. *Tectonophysics*, 344(3-4), 175-205. [https://doi.org/10.1016/S0040-1951\(01\)00271-2](https://doi.org/10.1016/S0040-1951(01)00271-2).

373

374Reiners, P. W., Zhou, Z., Ehlers, T. A., et al. 2003. Post-orogenic evolution of the Dabie Shan, eastern  
375 China, from (U-Th)/He and fission-track thermochronology. *American Journal of*  
376 *Science*, 303(6), 489-518. <https://doi:10.2475/ajs.303.6.489>.

377Regional geology of Shandong province. Geological Publishing House, Beijing, 1-595(in Chinese  
378 with English abstract).

379Regional geological map of Rushan 1:200000. Beijing: China Cartographic Publishing House, 1(in  
380 Chinese).

381Siebel, W., Danišik, M., Chen, F. 2009. From emplacement to unroofing: thermal history of the  
382 Jiazishan gabbro, Sulu UHP terrane, China. *Mineralogy and Petrology*, 96(3-4), 163-  
383 175. <https://doi:10.1007/s00710-009-0058-1>.

384Su, J., Zhu, W., Chen, J., et al. 2014a. Wide rift model in Bohai Bay Basin: Insight into the destruction  
385 of the North China Craton. *International Geology Review*, 56(5), 537-554.  
386 <http://www.tandfonline.com/loi/tigr20>.

387Su, J., Zhu, W., Chen, J., et al. 2014b. Cenozoic inversion of the East China Sea Shelf Basin:  
388 implications for reconstructing Cenozoic tectonics of eastern China. *International Geology*  
389 *Review*, 56(12), 1541-1555. <https://doi.org/10.1080/00206814.2014.951004>.

390Su, P., He, H., Tan, X., Liu, Y., Shi, F., Kirby, E. 2021. Initiation and Evolution of the Shanxi Rift  
391 System in North China: Evidence From Low-Temperature Thermochronology in a Plate  
392 Reconstruction Framework. *Tectonics*, 40(3), e2020TC006298.  
393 <https://doi.org/10.1029/2020TC006298>.

394Suo, Y., Li, S., Yu, S., et al. 2014. Cenozoic tectonic jumping and implications for hydrocarbon  
395 accumulation in basins in the East Asia Continental Margin: *Journal of Asian Earth Sciences*,  
396 88, 28-40. doi:10.1016/j.jseaes.2014.02.019.

397Sun, H., Li, H., Liu, L., et al. 2017. Exhumation history of the Jiaodong and its adjacent areas since  
398 the Late Cretaceous: Constraints from low temperature thermochronology. *Science China:*  
399 *Earth Sciences*, 60(3), 531-545. <https://doi:10.1007/s11430-016-0021-1>.

400Sun, Z., Zhu, H., Xu, C., et al. 2020. Reconstructing provenance interaction of multiple sediment  
401 sources in continental down-warped lacustrine basins: An example from the Bodong area,  
402 Bohai Bay Basin, China. *Marine and Petroleum Geology*, 113, 104142.  
403 <https://doi:10.1016/j.marpetgeo.2019.104142>.

404Shen, X., Tian, Y., Li, D., et al. 2016. Oligocene-Early Miocene river incision near the first bend of the  
405 Yangze River: Insights from apatite (U-Th-Sm)/He thermochronology. *Tectonophysics*, 687, 223-  
406 231. <https://doi.org/10.1016/j.tecto.2016.08.006>.

407Shu, L. Sh., Wang, B. Wang., L. Sh., et al. 2005. Analysis of Northern Jiangsu prototype basin from  
408 Late Cretaceous to Neogene. *Geological Journal of China Universities*, 11(4), 534-543(in  
409 Chinese with English abstract).

410Shuster, D. L., Flowers, R. M., Farley, K. A. 2006. The influence of natural radiation damage on  
411 helium diffusion kinetics in apatite. *Earth and Planetary Science Letters*, 249(3-4), 148-161.  
412 <https://doi.org/10.1016/j.epsl.2006.07.028>.

413Tan, M., Zhu, X., Liu, W., et al. 2018. Sediment routing systems in the second member of the Eocene  
414 Shahejie Formation in the Liaoxi Sag, offshore Bohai Bay Basin: A synthesis from tectono-  
415 sedimentary and detrital zircon geochronological constraints. *Marine and Petroleum*  
416 *Geology*, 94, 95-113. <https://doi:10.1016/j.marpetgeo.2018.04.003>.

417Tang, J., Zheng, Y. F., Wu, Y. B., et al. 2008. Zircon U–Pb age and geochemical constraints on the  
418 tectonic affinity of the Jiaodong terrane in the Sulu orogen, China. *Precambrian*  
419 *Research*, 161(3-4), 389-418. <https://doi.org/10.1016/j.precamres.2007.09.008>.

420Tang, Zh. B., Li, L. Shi, M. X. et al. 2011. Fission track thermochronology of Late Cretaceous -  
421 Cenozoic uplifting events of the Mengshan Mountain in the Western Shandong Rise, China.  
422 *Acta Scientiarum Naturalium Universitatis Sunyatseni*, 50(2), 127-133 (in Chinese with  
423 English abstract).

424Tarduno, J. A. 2007. On the motion of Hawaii and other mantle plumes. *Chemical Geology*, 241(3-4),  
425 234-247. <https://doi:10.1016/j.chemgeo.2007.01.021>.

426Vermeesch, P. 2010. HelioPlot, and the treatment of overdispersed (U-Th-Sm)/He data. *Chemical*  
427 *Geology*, 271(3-4), 108-111. <https://doi:10.1016/j.chemgeo.2010.01.002>.

428Wang, X., Zattin, M., Li, J., et al. 2013. Cenozoic tectonic uplift history of western Qinling: evidence  
429 from sedimentary and fission-track data. *Journal of Earth Science*, 24(4), 491-505.  
430 <https://doi:10.1007/s12583-013-0345-y>.

431Wang, Y., Wang, F., Wu, L., et al. 2018. (U-Th)/He thermochronology of metallic ore deposits in the  
432 Liaodong Peninsula: Implications for orefield evolution in northeast China. *Ore Geology*  
433 *Reviews*, 92, 348-365. <https://doi.org/10.1016/j.oregeorev.2017.11.025>.

434Wu, Zh. H., Wu, Zh. H. 2003. Low-temperature thermochronological analysis of the uplift history of  
435 the Yanshan Mountain and its neighboring area. *Acta Geologica Sinica*, 77(3), 399-406 (in  
436 Chinese with English abstract).

437Wu, Y. B., Zheng, Y. F. 2013. Tectonic evolution of a composite collision orogen: an overview on the  
438 Qinling-Tongbai-Hong'an-Dabie-Sulu orogenic belt in central China. *Gondwana*  
439 *Research*, 23(4), 1402-1428. <https://doi:10.1016/j.gr.2012.09.007>.

440Wu, L., Monié, P., Wang, F., et al. 2016. Cenozoic exhumation history of Sulu terrane: Implications  
441 from (U-Th)/He thermochronology. *Tectonophysics*, 672, 1-15.  
442 <https://doi:10.1016/j.tecto.2016.01.035>.

443Wu, L., Monie, P., Wang, F., et al. 2017. Multi-phase cooling of Early Cretaceous granites on the  
444 Jiaodong Peninsula, East China: evidence from  $^{40}\text{Ar}/^{39}\text{Ar}$  and (U-Th)/He  
445 thermochronology. *Journal of Asian Earth Sciences*, 160, 334-347.  
446 <https://doi.org/10.1016/j.jseaes.2017.11.014>.

447Wu, L., Shi, G., Danišik, M., et al. 2019. MK-1 Apatite: A New Potential Reference Material for (U-  
448 Th)/He Dating. *Geostandards and Geoanalytical Research*, 43(2), 301-315.  
449 <https://doi:10.1111/ggr.12258>.

450Wu, L., Wang, F., Yang, J., et al. 2020. Meso-Cenozoic uplift of the Taihang Mountains, North China:  
451 evidence from zircon and apatite thermochronology. *Geological Magazine*, 157(7), 1097-1111.  
452 <https://doi:10.1017/S0016756819001377>.

453Wu, L., Wang, F., Zhang, Z., et al. 2021. Reappraisal of the applicability of MK-1 apatite as a  
454 reference standard for (U-Th)/He geochronology. *Chemical Geology*, 120255.  
455 <https://doi.org/10.1016/j.chemgeo.2021.120255>.

456Xu, L. Q., Li, S. Zh., Guo, L. L. et al. 2016. Impaction of the Tan-Lu fault zone on uplift of the Luxi  
457 Rise: Constraints from apatite fission track thermochronology. *Acta Petrologica Sinica*, 32(4),  
458 1153-1170 (in Chinese with English abstract).

459Xu, W., Qiu, N., Chang, J., et al. 2020. Mesozoic-Cenozoic thermal evolution of the Linqing Sub-

460 basin, Bohai Bay Basin (eastern North China Craton): Constraints from vitrinite reflectance  
461 data and apatite fission track thermochronology. *Geological Journal*, 55(7), 5049-5061. <https://doi.org/10.1002/gj.3701>.

463 Yang, Q., Santosh, M., Shen, J. et al. 2014. Juvenile vs. recycled crust in NE China: Zircon U–Pb  
464 geochronology, Hf isotope and an integrated model for Mesozoic gold mineralization in the  
465 Jiaodong Peninsula. *Gondwana Research*, 25(4), 1445-1468.  
466 <https://doi.org/10.1016/j.gr.2013.06.003>.

467 Yang, R., Fellin, M. G., Herman, F., et al. 2016. Spatial and temporal pattern of erosion in the Three  
468 Rivers Region, southeastern Tibet. *Earth and Planetary Science Letters*, 433, 10-20.  
469 <https://doi.org/10.1016/j.epsl.2015.10.032>.

470 Yang, Z., Shen, C., Ratschbacher, L., et al. 2017. Sichuan Basin and beyond: Eastward foreland  
471 growth of the Tibetan Plateau from an integration of Late Cretaceous-Cenozoic fission track  
472 and (U-Th)/He ages of the eastern Tibetan Plateau, Qinling, and Daba Shan. *Journal of  
473 Geophysical Research: Solid Earth*, 122(6), 4712-4740.  
474 <https://doi.org/10.1002/2016JB013751>.

475 Yin, A. 2010. Cenozoic tectonic evolution of Asia: A preliminary synthesis. *Tectonophysics*, 488(1-4),  
476 293-325. <https://doi.org/10.1016/j.tecto.2009.06.002>.

477 Yu, J., Zheng, D., Pang, J., et al. 2019. Miocene Range Growth Along the Altyn Tagh Fault: Insights  
478 From Apatite Fission Track and (U-Th)/He Thermochronometry in the Western Danghenan  
479 Shan, China. *Journal of Geophysical Research: Solid Earth*, 124(8), 9433-9453.  
480 <https://doi.org/10.1029/2019JB017570>.

481 Zhao, R., Wang, Q., Liu, X., et al. 2018. Uplift history of the Jiaodong Peninsula, eastern North China  
482 Craton: implications for lithosphere thinning and gold mineralization. *Geological  
483 Magazine*, 155(4), 979-991. <https://doi.org/10.1017/S0016756816001254>.

484 Zhang, N. 2012. Comprehensive provenance study in sedimentary basin: an example from the  
485 Paleogene Dainan Formation of Gaoyou Depression, the North Jiangsu Basin. *Nanjing  
486 University*, 1-138(in Chinese with English abstract).

487 Zhang, W. B., Wu, L., Wang, F. 2016. Factors impacting the accuracy of apatite(U-Th)/He dating.  
488 *Seismology and Geology*, 38(4), 1107-1123(in Chinese with English abstract).

489 Zhang, Y. P., Zheng, W. J., Wang, W. T., et al. 2020. Rapid Eocene Exhumation of the West Qinling  
490 Belt: Implications for the Growth of the Northeastern Tibetan Plateau. *Lithosphere*, 2020(1), 1-  
491 12. <https://doi.org/10.2113/2020/8294751>.

492 Zhang, J., Wang, Y., Zhang, B., Qu, J., Li, J., Long, Y., Hui, J. 2021. Tectonothermal events in the  
493 central North China Craton since the Mesozoic and their tectonic implications: Constraints  
494 from low-temperature thermochronology. *Tectonophysics*, 228769.  
495 <https://doi.org/10.1016/j.tecto.2021.228769>.

496 Zheng, Y. 2008. A perspective view on ultrahigh-pressure metamorphism and continental collision in  
497 the Dabie-Sulu orogenic belt. *Chinese Science Bulletin*, 53(20), 3081-3104.  
498 <https://doi.org/10.1007/s11434-008-0388-0>.

499 Zhou, Z. Y. 2015. Low temperature thermochronology: Principles and Applications. *Science Press*,  
500 Beijing, 1-230 (in Chinese with English abstract).

501 Zhu, R., Xu, Y. 2019. The subduction of the west Pacific plate and the destruction of the North China  
502 Craton. *Science China: Earth Sciences*, 62(9), 1340-1350. <https://doi.org/10.1007/s11430-018->

- 503 9356-y.
- 504 Zhu, R. X., Zhu, G. Li, J. W. 2020. The North China Craton destruction. *Science Press*, 1-417 (in  
505 Chinese with English abstract).
- 506 Zhu, X., Shen, C., Zhou, R., et al. 2020. Paleogene sediment provenance and paleogeographic  
507 reconstruction of the South Yellow Sea Basin, East China: Constraints from detrital zircon U-  
508 Pb geochronology and heavy mineral assemblages. *Palaeogeography, Palaeoclimatology,*  
509 *Palaeoecology*, 553, 109776. [https://doi:10.1016/j.palaeo.2020.109776](https://doi.org/10.1016/j.palaeo.2020.109776).
- 510 包汉勇, 郭战峰, 张罗磊, 等. 2013. 太平洋板块形成以来的中国东部构造动力学背景. *地球科学进*  
511 *展*, 28(3), 337-346.
- 512 陈安定, 郭彤楼, 万景林. 2004. 裂变径迹、同位素年龄研究苏皖周边隆起构造抬升. *大地构造与*  
513 *成矿学*, 28(4), 379-387.
- 514 陈亮, 刘振湖, 金庆焕, 等. 2008. 北黄海盆地东部坳陷中生代构造演化. *大地构造与成矿学*,  
515 32(18), 308-316.
- 516 郭敬辉, 陈福坤, 张晓曼, 等. 2005. 苏鲁超高压带北部中生代岩浆侵入活动与同碰撞-碰撞后构造  
517 过程: 锆石 U-Pb 年代学. *岩石学报*, 21(4), 1281-1301.
- 518 胡圣标, 郝杰, 付明希, 等. 2005. 秦岭-大别-苏鲁造山带白垩纪以来的抬升冷却史—低温年代学  
519 数据约束. *岩石学报*, 21(4), 1167-1173.
- 520 李理, 钟大赉, 陈霞飞, 等. 2018. 鲁西地块 NW 走向断层的活动特征及裂变径迹证据. *地质学报*,  
521 92(3), 413-436.
- 522 李增达, 于晓飞, 王全明, 等. 2018. 胶东三佛山花岗岩的成因: 成岩物理化学条件, 锆石 U-Pb 年  
523 代学及 Sr-Nd 同位素约束. *岩石学报*, 34(2), 447-468.
- 524 林旭, 刘静. 2019. 江汉和洞庭盆地与周缘造山带盆山耦合研究进展. *地震地质*, 41(2), 499-520.
- 525 庞玉茂, 郭兴伟, 韩作振, 等. 2018. 南黄海中部隆起晚白垩世以来地层剥蚀的磷灰石裂变径迹分  
526 析. *地球科学*, 43(6), 1921-1930.
- 527 邱燕, 王立飞, 黄文凯. 2016. 中国海域中生代沉积盆地. 地质出版社, 北京, 1-233.
- 528 乳山 1:20 万区域地质图. 北京: 中国地图出版社, 1.
- 529 山东省区域地质志. 地质出版社, 北京, 1-595.
- 530 舒良树, 王博, 王良书, 等. 2005. 苏北盆地晚白垩世-新近纪原型盆地分析. *高校地质学报*, 11(4),  
531 534-543.
- 532 唐智博, 李理, 时秀朋, 等. 2011. 鲁西隆起蒙山晚白垩世-新生代抬升的裂变径迹证据. *中山大学学*  
533 *报(自然科学版)*, 50(2), 127-133.
- 534 吴中海, 吴珍汉. 2003. 燕山及邻区晚白垩世以来山脉隆升历史的低温热年代学证据. *地质学报*,  
535 77(3), 399-406.
- 536 许立青, 李三忠, 郭玲莉, 等. 2016. 郯庐断裂带对鲁西隆升过程的影响: 磷灰石裂变径迹证据. *岩*  
537 *石学报*, 32(4), 1153-1170.
- 538 张妮. 2012. 沉积盆地的物源综合研究-以苏北盆地高邮凹陷古近系戴南组为例. *南京大学*, 1-138.
- 539 张炜斌, 吴林, 王非. 2016. 磷灰石(U-Th)/He 年龄准确度的影响因素. *地震地质*, 38(4), 1107-1123.
- 540 中国地质调查局. 2004. 中华人民共和国地质图 1:250 万说明书. 北京: 中国地图出版社, 1.
- 541 周祖翼. 2015. 低温热年代学: 原理与应用. 科学出版社, 北京, 1-230.
- 542 朱日祥, 朱光, 李建威. 2020. 华北克拉通破坏. 科学出版社, 1-417.